

Performance of Corrosion-Damaged RC Columns Repaired by CFRP Sheets

by S.-W. Bae, A. Belarbi, and J.J. Myers

Synopsis: This study aimed to investigate the effectiveness of CFRP sheet in inhibiting the corrosion process of steel reinforcement embedded in RC columns. A total of 30 small-scale RC columns were conditioned under the accelerated corrosion process and then tested under uni-axial compression up to failure. Some of the columns were strengthened with CFRP sheets prior to the beginning of the accelerated corrosion process to simulate newly constructed RC columns wrapped with CFRP sheets. The others were strengthened with CFRP sheets after a certain period of the accelerated corrosion process to duplicate the corrosion-damaged RC columns to be repaired by wrapping with CFRP sheets. During the accelerated corrosion process, corrosion rate was monitored. The test results showed that although CFRP sheet wrapping decreased the corrosion rate, the corrosion of steel reinforcement could continue to occur. Based on the small-scale RC column tests, design guidelines were proposed and the proposed design guidelines were validated through test results of 4 mid-scale RC columns. The proposed design guidelines introduced a concept of equivalent area to account for the corrosion-damage such as internal cracking and cross-sectional loss of steel reinforcement.

Keywords: axial compressive capacity; CFRP sheets; corrosion; RC columns; repair

1448 Bae et al.

Sang-Wook Bae, ACI member, is a Post-Doctoral Research Fellow at the University of Missouri-Rolla. He received his BS and MS from Myongji University in South Korea and PhD from the University of Missouri-Rolla. His research interests include durability aspect of reinforced concrete structures including corrosion of steel reinforcement, and use of fiber-reinforced polymer composite materials in structural repair and rehabilitation

Abdeljelil Belarbi, FACI, is Distinguished Professor at the University of Missouri-Rolla. His research interests include constitutive modeling of reinforced and prestressed concrete as well as use of advanced materials and smart sensors in civil engineering infrastructures. He is a member of joint ACI-ASCE committees 445, and ACI Committees 440. He is Chair of subcommittee 445-5 (torsion of structural concrete).

John J. Myers, ACI member, is an Assistant Professor at the University of Missouri-Rolla. He received his BAE from The Pennsylvania State University; MS and Ph.D. from University of Texas-Austin. He is a member of ACI Committees 201, 342, 363, 440, E801, E802, and E803. His research interests include high performance concrete and use of fiber-reinforced polymers in structural repair and strengthening applications.

INTRODUCTION

Premature failure of RC structures due to corrosion of steel reinforcement is a significant problem. Particularly, with the extensive use of de-icing salt in cold weather regions, key bridge components, such as bridge decks and bridge piers, are vulnerable to corrosion of steel reinforcement. However, the conventional repair method consists of removing damaged concrete cover and patching low permeable materials, but this method has several limitations. Load transfer and structural issue is one of the problems of the conventional method. Removing the corrosion damaged concrete cover causes load redistribution and the exposed steel reinforcement may buckle and lose its capacity. Thus, a support system and complete traffic interruption are required during the repair process. Furthermore, it is common to see second and even third generation repairs if the structure remains in the same corrosive environment after repair. Consequently, engineers are looking for an innovative and cost-effective repair solution.

Strengthening of RC columns by wrapping with FRP composite materials has been widely studied over the past decade and the performance was verified through many laboratory tests and field applications. Wrapping an RC column with FRP composite sheets has also been tested to evaluate the applicability of the technology for the repair of corrosion damaged RC columns.¹ This is because FRP composite wraps have been thought to serve as diffusion barrier to inhibit the ingress of chloride ions, oxygen and moisture into the inside concrete, eventually decreasing the post-repair corrosion rate.

However, the effect of FRP composite sheet wrapping on the corrosion process has not yet been fully investigated. Although the wraps may reduce the ingress of new chloride ions and moisture into the inside concrete, they may also trap the existing moisture and ions. In addition, there is a possibility that chloride ions, moisture, and oxygen may ingress inside concrete through the unwrapped portion, resulting in

continuous corrosion. Once an RC column is wrapped with FRP composite sheets, it is impossible to detect the symptoms of the continuous corrosion using the currently available non-destructive corrosion monitoring techniques such as the half-cell potential method and the polarization measurement method.²

The objectives of this research project were twofold: (1) to investigate the effectiveness of FRP sheet wrapping for the repair of corrosion damaged RC columns through laboratory tests; (2) to propose design guidelines for the corrosion damaged RC columns repaired by FRP sheet wrapping based on the obtained test results.

RESEARCH SIGNIFICANCE

Although the effectiveness of the repair/rehabilitation of RC columns by CFRP sheet wrapping has been widely investigated, the information on the long-term behavior of RC columns wrapped with CFRP sheets including the continuous corrosion process are limited. This study verified the long-term performance of RC columns wrapped with CFRP sheets under severe corrosive environment, and suggested design guidelines. The proposed design guidelines included strength reduction factors to account for the damage induced by corrosion of steel reinforcement.

EXPERIMENTAL PROGRAM

The experimental program included two different scales of RC columns; (1) small-scale and (2) mid-scale RC columns. A total of 30 small-scale RC columns were tested for a comprehensive parametric study. Based on the results of small-scale tests, design guidelines for the corrosion-damaged RC columns repaired by FRP sheet wraps were proposed. The proposed design guidelines were evaluated through comparison with the test results of 4 mid-scale RC columns.

Figure 1 presents the specimen details of small-scale RC columns. The diameter of the columns is 152 mm and the height is 457 mm. Deformed reinforcing bars with a diameter of 9.5 mm and the nominal yield strength of 414 MPa were used as longitudinal reinforcement. Steel wires with a diameter of 3.7 mm were used as spiral reinforcement. Figure 2 shows the steel cage used for small-scale RC columns. As shown in Figure 2, the spiral reinforcement and the longitudinal reinforcement located around the spiral acted as the anode during the accelerated corrosion process while the longitudinal reinforcement at the center of the column acted as the cathode. In addition, electric connections were made at the end of the longitudinal reinforcement to accelerate the corrosion process. The concrete used in this study was produced according to the mixture proportion as shown in Table 1. The mixture proportion was designed to produce concrete with higher permeability so that moisture and ions can easily ingress into concrete, eventually accelerating the corrosion process in the laboratory. The concrete strength was 21 MPa at the time of testing.

MbraceTM CF High Tensile Carbon Fiber sheets (CFRP sheet hereafter) were used to strengthen the columns. The tensile strength and the elastic modulus of the sheet

were 3790 MPa and 228 GPa, respectively.³ The CFRP sheets were applied using epoxy-based resins, namely, MbraceTM primer and saturant. Figure 2 presents the picture small-scale RC columns after CFRP sheet wrapping. Detailed procedure of CFRP sheet application using the epoxy-base resin, a so called wet lay-up technique, can be found in the above mentioned reference.³

The accelerated corrosion process was achieved by wet-dry cycles and imposing electric potential between the anode and cathode reinforcement as shown in Figure 3; the columns were placed in the water tank filled with 5 % saline solution to simulate wet-dry cycles and destroy the passive film of steel reinforcement. Fixed electric potential of 6 V was applied between the anode and cathode reinforcement using a DC power supply during the wet-dry cycles. Corrosion rate was monitored by measuring the electric current between the anode and cathode reinforcement using a voltmeter and 1 Ω resistor.

A total of 30 small-scale RC columns were tested as summarized in Table 2. Column CONT was used as the control column and was kept at room temperature until testing. Columns CON2 and CON3 were conditioned by wet-dry cycles using 5 % saline solution. The purpose of these columns was to simulate the natural corrosion process of RC columns under severe corrosive environment.

Column CON4 was not strengthened with CFRP wraps but conditioned under the accelerated corrosion process to serve as corrosion-damaged RC columns. Columns CFRP1, CFRP2, CFRP3 and CFRP4 were strengthened with CFRP sheets and were conditioned under the accelerated corrosion process; Columns CFRP1 and CFRP3 were strengthened with CFRP sheets before the start of the accelerated corrosion process, while Columns CFRP2 and CFRP4 were strengthened after the accelerated corrosion process to induce corrosion-damage. In addition, micro-cracks between fibers and matrix may develop due to the freeze-thaw cycles, eventually resulting in an increase in corrosion rate because of the moisture ingress through the micro-cracks. Thus, Columns CFRP3 and CFRP4 were conditioned under the 300 non-moist freeze-thaw cycles; the test programs of Columns CFRP3 and CFRP4 are identical to those of the columns CFRP1 and CFRP2, respectively, except for the freeze-thaw cycles. One freeze-thaw cycle consisted of one-hour freeze at 0 °F and one-hour thaw at 50 °F, and 30 min. ramping up and down. Once the accelerated corrosion process was completed, uni-axial compression tests were conducted in order to evaluate the change of the mechanical properties such as axial compression capacities, axial stiffness, and ductility.

Figure 4 shows the specimen detail of mid-scale RC columns, which may represent 1/4 scale of RC columns. The mid-scale RC columns consisted of a circular column and concrete blocks to simulate bridge piers and cap beams. Ready-mixed concrete was used and the strength was 34 MPa. As shown in Figure 4, the height of mid circular column was 914 mm and the diameter was 203 mm. Eight deformed reinforcing bars with a diameter of 9.5 mm made the longitudinal reinforcement. Reinforcing bars with a diameter of 6.4 mm were used as spiral reinforcement. The nominal yield strength of the reinforcing bars was 414 MPa. Aluminum pipes, made of Aluminum 6061-T6,

were used as an internal cathode for the accelerated corrosion process as shown in Figure 4.

One layer of CFRP sheet was applied along the height of the circular column using the wet lay-up technique. The accelerated corrosion process was achieved using the cathode made of aluminum pipe as shown in Figure 4. The aluminum pipe had drilled holes along the length of the pipe so that the moisture and ions necessary for the corrosion process can be easily supplied to the cathode and inside concrete. The electric potential of 6 V was imposed during the accelerated corrosion process between the anode reinforcement and the cathode aluminum pipe. The corrosion rate was monitored by measuring the electric current between the two electrodes.

A total of 4 mid-scale RC columns were tested as summarized in Table 3. Column CFRP-COR was strengthened with CFRP sheet wrapping before the beginning of the accelerated corrosion process. Columns COR-CFRP and COR-CFRP-COR were conditioned first under the accelerated corrosion process and then strengthened with the CFRP sheet wraps. However, Column COR-CFRP-COR was conditioned again under the accelerated corrosion process after it was strengthened with the CFRP sheet wrapping. Columns CFRP-COR and COR-CFRP were conditioned under 300 freeze-thaw cycles before failure tests. The profile of the freeze-thaw cycles is the same as that in used in small-scale tests. Column COR-CFRP-COR was freeze-thaw conditioned after CFRP wrapping and then conditioned again under the accelerated corrosion process.

After completion of the accelerated corrosion process, uni-axial compression failure tests were carried out in order to evaluate the change of the mechanical properties due to the corrosion of steel reinforcement.

TEST RESULTS AND DISCUSSIONS

Results of accelerated corrosion process

Figure 5 shows the steel weight loss of the reinforcement at the anode side vs. time curves of the unwrapped columns CON4 and the CFRP wrapped columns CFRP1. The steel weight loss was estimated using Faraday's Law and the electric current measured during the accelerated corrosion process as shown in Equation (1):

$$w(g) = \frac{A_m}{z \cdot F} \sum \Delta t \cdot I_{ave} \quad (1)$$

where, $w(g)$ is accumulated steel loss (grams), A_m is atomic mass (for iron 55.85 g), I_{ave} is average current (Amp) applied over time increment Δt (second), z is valency (assuming that most of rust product is $\text{Fe}(\text{OH})_2$, it is taken as 2), and F is Faraday's constant (96487 C/eq). In Equation (1), it was assumed that all of the current resulting from the accelerated corrosion process is used to produce rust.

As shown in Figure 5, the average corrosion rate of unwrapped columns CON4 during the first stage of the accelerated corrosion process (wet-dry cycles) was 4.51 g/day while that of CFRP wrapped columns CFRP1 was 1.55 g/day. However, during the

second stage of the accelerated corrosion process (dry condition), the corrosion rate of the unwrapped columns CON4 significantly decreased up to 0.68 g/day while the decreasing rate of the corrosion rate of the CFRP wrapped columns CFRP1 was significantly smaller as compared to the unwrapped columns. These results imply that even if RC columns were wrapped with CFRP sheets, corrosion could occur. This is due to the fact that the moisture and ions can ingress inside concrete by means of instantaneous absorption followed by diffusion through the matrix resin and the unwrapped portion of the columns. Furthermore, even if the external corrosion sources were removed (the second stage, dry condition, in Figure 5), the corrosion of steel reinforcement in CFRP wrapped columns may continue to occur since the evaporation of the entrapped moisture is inhibited. Similar results were reported by other studies.^{1,4}

During the accelerated corrosion process, hoop strains of CFRP wraps were measured using strain gages. The measured hoop strains vs. percentile loss of cross-sectional area of steel reinforcement are presented in Figure 6. As shown in Figure 6, the hoop strains were not increased until the percentile loss of steel reinforcement reached 5%. After that, the hoop strains exhibited a rapid increase up to 20% loss of the cross-sectional area. This may imply that the hoop strain did not increase until the rust, which is a by-product of the corrosion process, filled in the void of concrete. Once the void was filled with the rust, concrete started to expand, causing the internal pressure into CFRP wraps.

In order to investigate the internal damage due to the internal pressure induced by the corrosion process, cross-sectional cuts were taken as shown in Figure 7. As a result, it was found that even if RC columns were wrapped with CFRP sheets, cracks developed due to the corrosion of steel reinforcement along the longitudinal and spiral reinforcement which acted as the anode during the accelerated corrosion process. However, the crack widths of the CFRP wrapped columns (CFRP1 through CFRP4) were relatively smaller when compared to the unwrapped column (CON4) as shown in Table 4. Due to this internal damage, the behavior of the small-scale RC columns observed during the failure tests under the uni-axial compression was significantly reduced.

Results of compression tests

Uni-axial compression tests were conducted after completion of the accelerated corrosion process, and the obtained failure load and failure modes are summarized in Table 5. The failure of unwrapped columns occurred due to the cracking and spalling of the concrete cover as shown in Figure 8. However, it was noticed that the spalling of the concrete cover of the corrosion-damaged unwrapped columns (CON4) occurred along the height of the columns almost at the same time, showing the significant loss of failure load as compared to the control columns (CONT; control column of the unwrapped columns). This is probably because the concrete cover of the unwrapped columns were already delaminated, prior to the failure tests, due to the cracks formed around the spiral reinforcement as previously discussed. The columns wrapped with CFRP sheets before the start of the accelerated corrosion process (CFRP 1 and CFRP3) and their control column (CON3; control column of the CFRP wrapped columns) failed directly due to the rupture of CFRP sheet as shown in Figure 8. However, the failure of the columns

wrapped with CFRP sheets after the accelerated corrosion process (i.e., these columns were already corrosion-damaged before CFRP wrapping) were mainly due to the lap splice debonding, causing the decrease in failure load.

Comparing the unwrapped corrosion-damaged column (CON4) and its corresponding control column (CONT), it was clearly shown that the axial compression capacity was significantly decreased due to the corrosion damages such as cracking and cross-sectional loss of steel reinforcement. However, the axial capacity of corrosion damaged columns could be restored by CFRP sheet wrapping; the failure load of the columns, damaged by the accelerated corrosion process but strengthened with CFRP wraps (CFRP2 and CFRP4), was significantly higher than the unwrapped corrosion-damaged column (CON4).

By comparing the control column of CFRP wrapped columns (CON3) and CFRP wrapped columns conditioned under the accelerated corrosion process (CFRP1 through CFRP4), it was found that the failure load of CFRP wrapped columns was slightly decreased. One reason for the decrease in the failure load is definitely attributed to the internal damages such as concrete cracking and cross-sectional loss of steel reinforcement; while the other reason could be due to the decrease in the ultimate tensile strain of CFRP sheet.

Internal damage such as concrete cracking, and cross-sectional loss of steel reinforcement changed the axial compressive behavior of the CFRP wrapped columns. Figure 9 presents the axial load vs. axial strain curves of the test columns. As shown in Figure 9, the initial axial rigidity (EA), which can be defined as the initial linear slope of the curves, decreased due to the accelerated corrosion process as compared to their control column CON3 that was wrapped with CFRP sheets and not treated with the accelerated corrosion process. In other hand, the second linear slope beyond the transition zone was almost not affected as shown in Figure 9.

In fact, the initial axial rigidity of RC columns is almost not significantly affected by CFRP wrapping because of the passive characteristic of CFRP wrapping system. In other words, the CFRP wrapping has no significant effect on the initial behavior of columns. Thus, if there is a change in the initial behavior, it would be due to the change in either concrete or steel reinforcement. In this study, the change in initial behavior was observed as the decrease in the initial axial rigidity of the columns. It was therefore assumed that the decrease was caused by the cracking and spalling of cover concrete (even if RC columns are wrapped with CFRP sheets) and the loss of steel reinforcement, eventually resulting in the decrease of the effective cross-sectional area. It should be noted that this assumption was on the basis that the elastic modulus of concrete is not affected by the corrosion process. The internal cracking of concrete inside CFRP wrapping due to the corrosion process was clearly observed by cutting off the cross-section of the columns after the accelerated corrosion process. In order to quantify the degradation of concrete due to the cracking and the loss of steel, a concept of equivalent area was evaluated. The equivalent area A_{eqv} can be defined as,

$$A_{eqv} = \phi_{cor2} [A_g - (A_{st})_{cor}] = \phi_{cor2} (A_g - \phi_{cor1} A_{st}) \quad (2)$$

where, A_{eqv} is equivalent area, A_g is gross area, A_{st} is area of steel reinforcement, $(A_{st})_{cor}$ is reduced area of steel reinforcement due to corrosion, ϕ_{cor1} is an area reduction factor to account for the steel loss due to corrosion, and ϕ_{cor2} is an area reduction factor to account for the degradation of concrete due to cracking caused by corrosion of steel reinforcement.

Area reduction factors, ϕ_{cor1} and ϕ_{cor2} , were experimentally determined in this study. The area reduction factor, ϕ_{cor1} , is actually the ratio of the reduced area of steel reinforcement after corrosion process to the original area. Thus, it was determined using the steel weight loss calculated by Faraday's Law. The area reduction factor, ϕ_{cor2} , was calculated based on the test results of small-scale tests using the following equation,

$$\phi_{cor2} = \frac{P_u - f_s A_{st}}{(P_u - f_s A_{st})_{control}} = \frac{f'_c A_{eqv}}{(f'_c A_{eqv})_{control}} \quad (3)$$

where, P_u is ultimate load, f_s is stress of longitudinal reinforcement, A_{st} is area of longitudinal reinforcement, and f'_c is concrete. Figure 10 presents The relationship between the area reduction factors ϕ_{cor1} and ϕ_{cor2} calculated using Equation (3).

Figure 11 shows the ratio of the measured tensile strain of CFRP wraps, ϵ_{total} , and the ultimate tensile strain provided by the manufacturer, ϵ_{fu} . In Figure 11, ϵ_{total} is the sum of the hoop strain due to the mechanical loading at failure during the failure test and the hoop strain caused by the expansion of concrete measured at the end of the accelerated corrosion process.

For control columns, the measured strain, ϵ_{total} , of Column CON3, which was wrapped with CFRP sheet but not conditioned under the accelerated corrosion process, was about 60 % of the ultimate tensile strain provided by the manufacturer, ϵ_{fu} , as shown in Figure 11. There are several reasons for that. First, in spite of using the same materials, the process of making flat coupons, which is usually used to obtain the ultimate tensile strain and strength by manufacturers, is easier than that of making the FRP wrapping system. As a result, the FRP composite in the form of a flat coupon may have a higher quality than the FRP wrapping system. Second, due to the existence of the internal pressure acting on the surface of the FRP sheet, as well as the axial stress in the FRP sheets transferred by the bond between the concrete and FRP sheets, the FRP sheets are in a tri-axial stress state instead of pure tension as in the flat coupon test. Finally, cracking and crushing of the concrete core inside the FRP sheet cause local stress concentrations in the various locations of the FRP sheet. However, it should be noted that the hoop strains of CFRP wraps were measured using strain gages and thus, the measured strain might be localized strains. Thus, the actual rupture strain at failure might

be greater than the measured strains. Similar results were reported that the measured ultimate tensile strains were 50 to 80 % of the ultimate tensile strains provided by the manufacturer.⁵ In order to consider this reduction in ultimate tensile strain in the design, it is suggested that the material properties of the CFRP sheet be calculated as,

$$\varepsilon_{fu}^* = R_c \varepsilon_{fu} \quad (4)$$

$$f_{fu} = E_f \varepsilon_{fu}^* \quad (5)$$

where, ε_{fu}^* is design ultimate tensile strain of FRP sheets, R_c is reduction factor, ε_{fu} is ultimate tensile strain provided by the manufacturer, f_{fu} is design tensile strength of FRP sheet and E_f is elastic modulus of CFRP sheets. These material properties should be used to calculate the concrete strength confined by CFRP wraps. The reduction factor, R_c was determined as 0.5 based on the test results and details reported by authors elsewhere.⁶

However, as the steel reinforcement lost the cross-sectional area, that is, rust was produced, CFRP wraps was pre-stressed due to the expansion of the inside concrete, resulting in the reduction of the ultimate tensile strain of CFRP wraps. As a result, in the case where the CFRP wrapped columns were conditioned under the accelerated corrosion process, the measured rupture strain due to the mechanical loading was significantly reduced since the CFRP wraps were prestressed during the accelerated corrosion process as shown in Figure 11. Equation (4) should be modified in case of CFRP wrapped RC columns placed in corrosive environment, as follows,

$$\varepsilon_{fu}^* = R_c \varepsilon_{fu} - (\varepsilon_r)_{corrosion} \quad (6)$$

where, $(\varepsilon_r)_{corrosion}$ is pre-strain induced by the corrosion of steel reinforcement.

In the case of freeze-thaw effect, it was found that the cross-sectional loss of the steel reinforcement of the columns conditioned by freeze-thaw cycles was slightly greater than that of the unconditioned columns. In addition, the equivalent area calculated by Equation (2) of the freeze-thaw conditioned columns was slightly smaller as compared to the unconditioned columns, consequently resulting in the decrease in failure load. Thus it can be hypothesized the freeze-thaw cycles caused micro-cracking in the CFRP wraps so that moisture could ingress through the cracks. To verify this phenomenon, microscopic investigation is necessary.

PROPOSED DESIGN GUIDELINES

Axial compressive capacity of RC spiral columns wrapped with CFRP sheets under corrosive environment can be determined as follows;

$$\phi P_n = 0.85\phi \left[0.85\psi_f f'_{cc} A_{eqv} + f_y (A_{st})_{cor} \right] \quad (7)$$

where, ϕ is code reduction factor, ψ is strength reduction factor proposed by ACI Committee 440 to account for the uncertainty of new technology,⁷ taken as 0.95, and f'_{cc} is concrete strength confined with FRP sheets. The equivalent area, A_{eqv} , and reduced area of steel reinforcement, $(A_{st})_{cor}$, can be determined using the area reduction factors, ϕ_{cor1} and ϕ_{cor2} as shown in Equation (2).

In order to determine the area reduction factors, ϕ_{cor1} and ϕ_{cor2} , the area reduction factor ϕ_{cor2} of small-scale RC columns were calculated and the corresponding experimental results are summarized in Table 6. Based on the results shown in Table 6, area reduction factors, ϕ_{cor1} and ϕ_{cor2} , for four RC columns exposed to four different categories of environmental conditions are proposed and summarized in Table 7. For instance, Column CFRP1 as shown in Table 6 was strengthened with CFRP sheets and then conditioned under the accelerated corrosion process. Thus, Column CFRP1 could represent Case 1 in Table 7, newly constructed RC columns wrapped with CFRP sheets. In Table 7, area reduction factors, ϕ_{cor1} , were calculated using the relationship between ϕ_{cor1} and ϕ_{cor2} as shown in Figure 10.

Currently, many analytical models are available to determine concrete strength confined with FRP sheets, f'_{c} . In this study, the model previously developed by the authors was used in Equation (6).⁶ The model was proven to be reasonably accurate to estimate concrete strength confined by FRP sheets within less than 10 % prediction error. However, it is not the intention of this paper to discuss the details of the analytical model. The purpose of this paper is to re-evaluate the concept of equivalent area to account for the corrosion damage to RC columns wrapped with CFRP sheets. The performance of the proposed design guidelines were validated through comparison with the test results of mid-scale RC columns of which size, material properties, and confinement level were different from small-scale RC columns used for the development of the proposed design guidelines. For comparison purpose, all the strength reduction factors in Equation (4) were excluded when calculating the axial compressive capacity of mid-scale RC columns. The comparison between predictions and experimental results are presented in Table 8. The area reduction factors for mid-scale columns were determined according to the test program applied to the columns; thus, CFRP-COR would correspond to Case 3, and COR-CFRP and COR-CFRP-COR to Case 4.

As shown in Table 8, the predicted values were about 20 % less than the experimental results in case of CFRP-COR and COR-CFRP. One major reason for the difference is due to the inaccuracy of the analytical model to calculate the concrete strength confined by FRP sheet. The other reason is probably because the area reduction factors were developed based on the test results of small-scale RC columns which simulated more severe corrosion damage than mid-scale RC column tests. In the case of COR-CFRP-COR, the failure of the columns was due to the lap splice debonding, resulting in significant loss of the axial compressive capacity as shown in Figure 12. As a result, the predicted value was about 42 % higher than the experimental result. Lap splice debonding failure was frequently observed if corrosion-damaged columns were strengthened with CFRP sheets and then re-conditioned by the accelerated corrosion process. Lap splice debonding was probably due to the pre-existed cracks along the

height of the columns; however, the failure mechanism has not been fully investigated, and needs further attention.

CONCLUSIONS

In this study, the effect of CFRP sheet wrapping on protection of RC columns from corrosion of steel reinforcement was investigated using small-scale and mid-scale RC columns and the following conclusions were made.

(1) Corrosion of steel reinforcement could continue to occur even if RC columns were wrapped with CFRP sheets. This was probably because moisture ingress into concrete by means of absorption followed by diffusion through matrix resin and the unwrapped portion. Furthermore, CFRP wraps inhibited the evaporation of entrapped moisture and ions, resulting in continuous corrosion.

(2) As a result of corrosion of steel reinforcement, internal cracks occurred as well as cross-sectional area of steel reinforcement reduced, eventually decreasing the initial axial rigidity of the columns. In order to consider these results in the design of RC columns wrapped with CFRP sheets, the concept of equivalent area was introduced.

(3) The rupture strain of CFRP sheets due to the mechanical loading was decreased due to the pre-strain caused by the expansion of concrete due to the corrosion of steel reinforcement. Thus, the design ultimate tensile strain of CFRP sheets should be reduced to account for this effect. Based on the test results of this study and the authors' previous study, an equation to determine design ultimate tensile strain was proposed.

(4) Design guidelines were proposed based on the test results of small-scale RC columns. The proposed guidelines included equations to determine the axial compression capacity of CFRP wrapped columns placed in corrosive environment. The performance of the guidelines appeared to be somewhat conservative since the guidelines were developed based on small-scale tests which simulate considerably severe corrosion damage that is not likely to exist in the field.

(5) The design factors proposed in this study need to be further refined since they were developed from the limited data obtained in this study. Thus, as a next step of this study, it is necessary to quantify the relationship between the level of corrosion of steel reinforcement and hoop strain of CFRP sheet and compare it to real life situation.

ACKNOWLEDGMENTS

This research was funded by the Missouri Department of Transportation and UMR University Transportation Center. Their financial support is gratefully acknowledged.

REFERENCES

1. Pantazopoulou, S. J., Bonacci, J. F., Sheikh, S., Thomas, M. D. A. and Hearn, N., "Repair of Corrosion-Damaged Columns with FRP Wraps," *Journal of Composites for Construction*, V. 5, No. 1, 2001, pp. 3-11.
2. Carino, N.J., "Nondestructive Techniques to Investigate Corrosion Status in Concrete Structures," *Journal of Performance of Constructed Facilities*, V. 13, No. 3, 1999, pp. 96-106.
3. Master Builders Inc., "Mbrace™ Composite Strengthening System-Engineering design guidelines; second edition," Cleveland, OH, 1998.
4. Okba, S. H., El-Dieb, A. S., El-Shafle, H. M. and Rashad, A., "Evaluation of Corrosion Protection for Reinforced Concrete Wrapped by FRP," *Proceedings of A New Era of Building (ICPCM2003)*, Cairo, Egypt, 2003.
5. Xiao, Y. and Wu, H., "Compressive Behavior of Concrete Confined by Carbon Fiber Composite Jackets," *Journal of Materials in Civil Engineering*, V. 12, No. 2, 2002, pp. 139-146.
6. Bae, S., "Evaluation of the Effects of Various Environmental Conditions on RC Columns Wrapped with FRP Sheets," *PhD Dissertation*, University of Missouri-Rolla, Rolla, MO, 2004.
7. ACI Committee 440, "Guide for the Design and Construction of Externally Bonded FRP Systems for Strengthening Concrete Structures," American Concrete Institute, Farmington Hills, Mich., 2002.

Table 1--Mixture proportion of concrete for small-scale tests [unit: kg/m³]

W/C	Cement	Water	Gravel	Sand	AE
0.62	290	178	756	1080	190 ml

Table 2--Test matrix for small-scale columns

Specimen	Test program*	Number of specimens
CONT	None-FA: Control	4
CON2	WD-FA	3
CON3	AF-CL-FA	3
CON4	[WD+FP]-FA	4
CFRP1	AF-[WD+FP]-FA	4
CFRP2	[WD+FP]-AF-[WD+FP]-FA	4
CFRP3	AF-[WD+FP]-FT-[WD+FP]-FA	4
CFRP4	[WD+FP]-AF-FT-[WD+FP]-FA	4

*Note: WD (Wet-Dry Cycles), FP (Fixed Electric Potential), [CL+FP] (Wet-Dry Cycles and Fixed Electric Potential Simultaneously), AF (Apply FRP Sheet), FT (Freeze-Thaw Cycles), and FA (Failure Test).

Table 3--Test matrix for mid-scale columns

Specimen	Test program*	NS**
CONT	None-FA: Control	1
CFRP-COR	AF-[WD+FP]-FT-FA	1
COR-CFRP	[WD+FP]-AF-FT-FA	1
COR-CFRP-COR	[WD+FP]-AF-FT-[WD+FP]-FA	1

*Note: WD (Wet-Dry Cycles), FP (Fixed Electric Potential), [CL+FP] (Wet-Dry Cycles and Fixed Electric Potential Simultaneously), AF (Apply FRP Sheet), FT (Freeze-Thaw Cycles), and FA (Failure Test).

**NS: number of specimens

Table 4—Measured crack width

Specimen	Circumferential*		Longitudinal*	
	[mm]	(COV %)	[mm]	(COV %)
CON4	0.71	(30)	0.94	(13)
CFRP1	0.30	(20)	0.23	(16)
CFRP2	0.38	(27)	0.64	(43)
CFRP3	0.33	(35)	0.25	(41)
CFRP4	0.58	(27)	0.38	(0)

* Average of three measurement at three different locations

Table 5--Failure loads and failure modes of small-scale RC columns

Specimen	Failure load*		Failure mode
	[kN]	(COV %)	
CONT	471.5	(5)	Concrete crushing
CON2	542.7	(2)	Concrete crushing
CON3	871.9	(3)	FRP rupture
CON4	293.6	(9)	Concrete crushing
CFRP1	774.0	(10)	FRP rupture
CFRP2	720.6	(7)	Lap splice debonding
CFRP3	747.3	(2)	FRP rupture
CFRP4	645.0	(5)	Lap splice debonding

* Average of three specimens

Table 6--Area reduction factors, ϕ_{cor2} of small-scale RC columns

Specimen	ϕ_{cor2}	Testing schemes
CONT	1.00	Control
CFRP1	0.93	CFRP sheets were applied before the accelerated corrosion process
CFRP2	0.86	CFRP sheets were applied as a repair method after the columns were severely damaged by corrosion
CFRP3	0.89	Same as CFRP1 but conditioned under freeze-thaw cycles after CFRP wrapping
CFRP4	0.76	Same as CFRP2 but conditioned under freeze-thaw cycles after CFRP wrapping

Table 7--Proposed area reduction factors, ϕ_{cor1} and ϕ_{cor2}

ϕ_{cor1}	ϕ_{cor2}	Environmental conditions
0.75	0.95	[Case 1] Newly constructed RC columns wrapped with CFRP sheet
0.65	0.85	[Case 2] Corrosion damaged RC columns repaired by CFRP wrapping
0.70	0.90	[Case 3] Newly constructed RC columns wrapped with CFRP sheet and placed where possible non-moist freeze-thaw damages are anticipated
0.55	0.75	[Case 4] Corrosion damaged RC columns repaired by CFRP wrapping, and placed where possible non-moist freeze-thaw cycles are anticipated

Table 8--Comparison of axial compressive capacity between predicted and experimental results

Specimen	Predictions [kN]	Experiments[kN]	Pred./Exp.
CFRP-COR	1557	1926	0.81
COR-CFRP	1348	1685	0.80
COR-CFRP-COR	1334	939	1.42

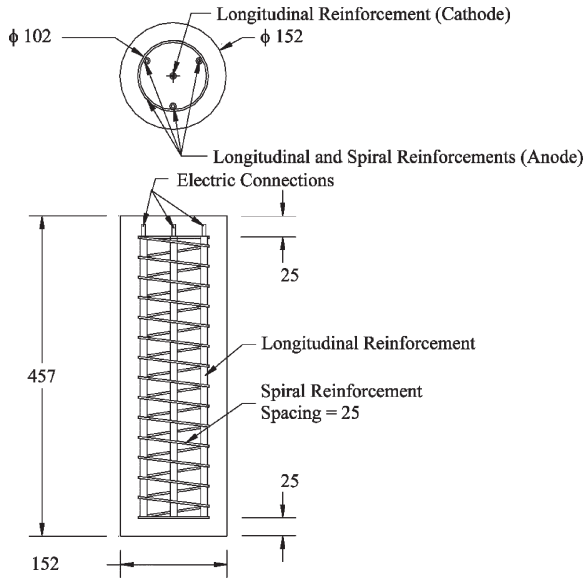


Figure 1—Specimen details of small-scale RC columns (dimensions in mm)

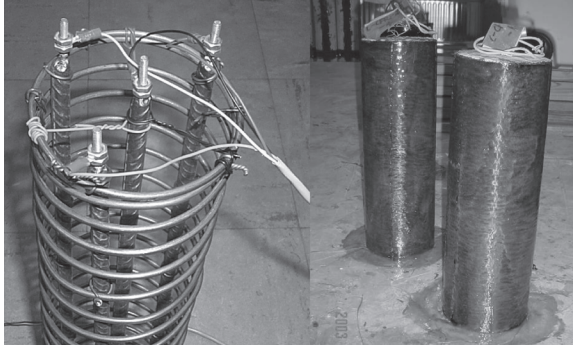


Figure 2—Reinforcement cage used for small-scale RC columns (left) and small-scale RC columns after CFRP sheet wrapping

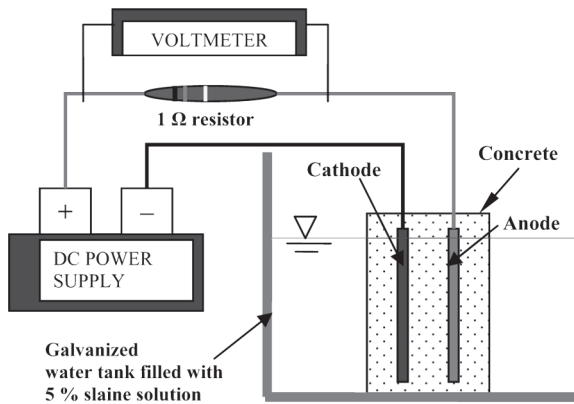


Figure 3—Schematic drawing of the accelerated corrosion process used in this study

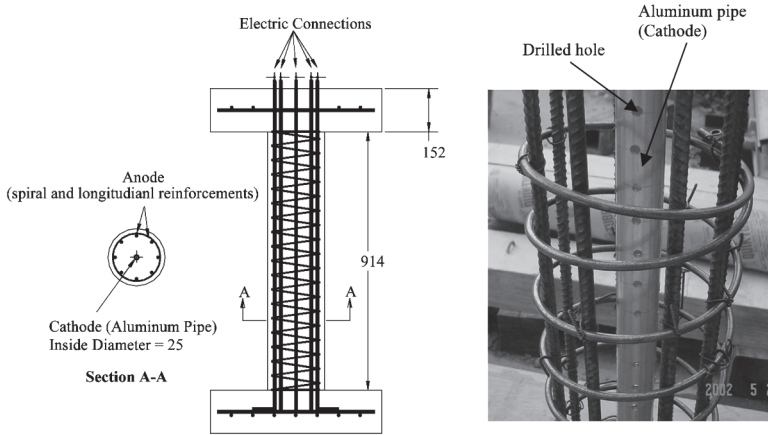


Figure 4—Specimen details of mid-scale RC columns and reinforcement cage used for mid-scale RC columns (dimensions in mm)

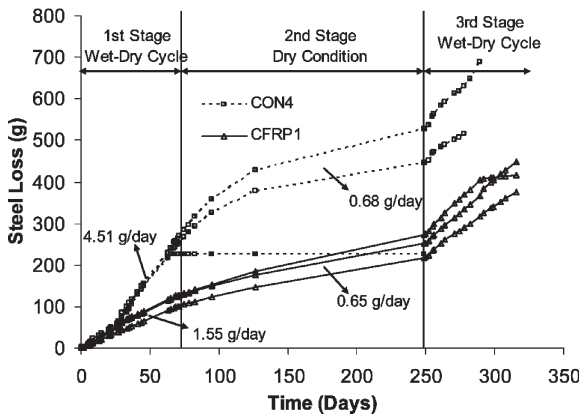


Figure 5—Steel weight loss vs. time curves of Columns CON₄ and CFRP₁

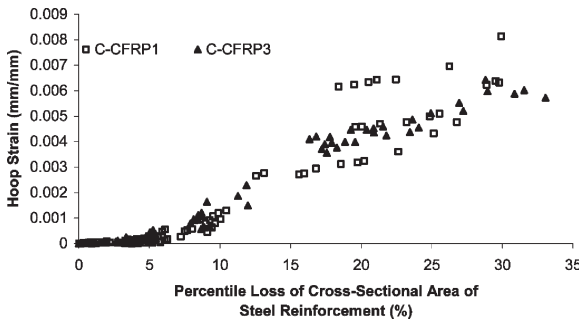


Figure 6—Hoop strain vs. percentile loss of cross-sectional area of steel reinforcement

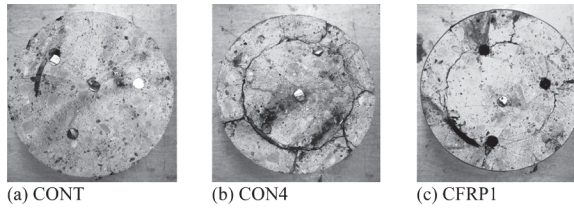


Figure 7—Internal damage due to corrosion of steel reinforcement

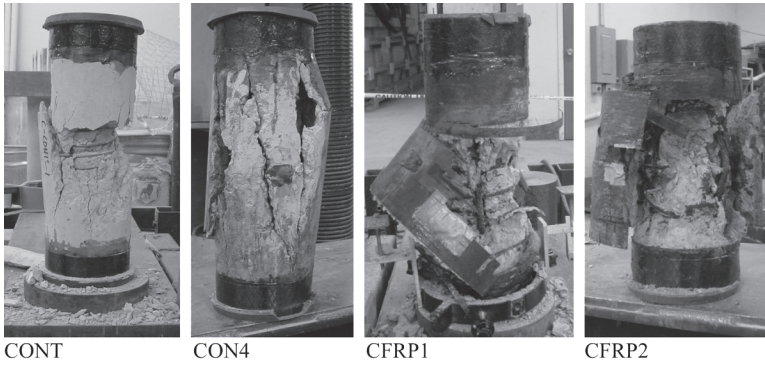


Figure 8—Failure modes of small-scale RC columns

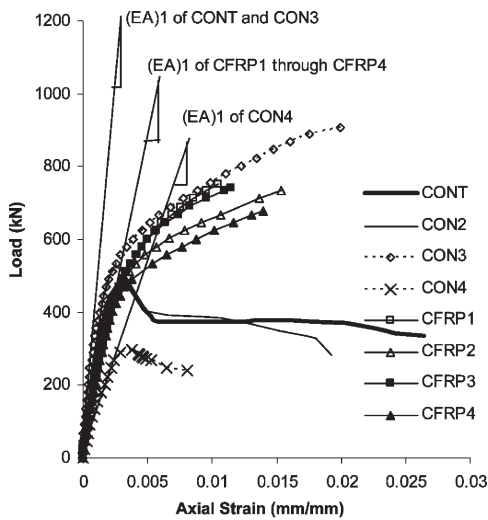


Figure 9—Axial load vs. axial strain curves of all columns

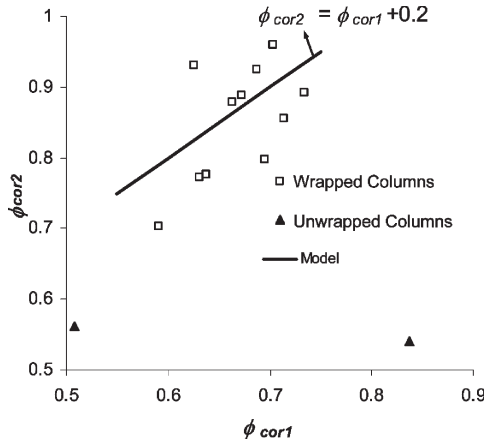


Figure 10—Relationship between ϕ_{cor1} and ϕ_{cor2}

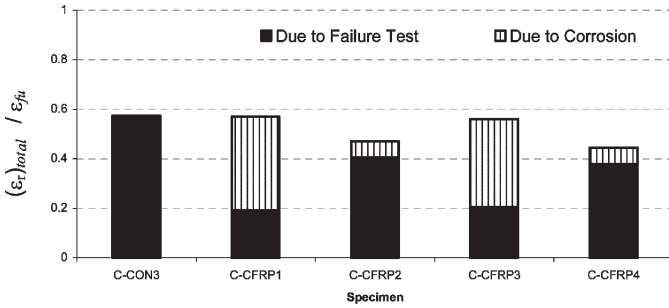


Figure 11—Ratio of the measured ultimate tensile strain of FRP wraps (ϵ_{total}) and the ultimate tensile strain (ϵ_{fu}) provided by the manufacturer.

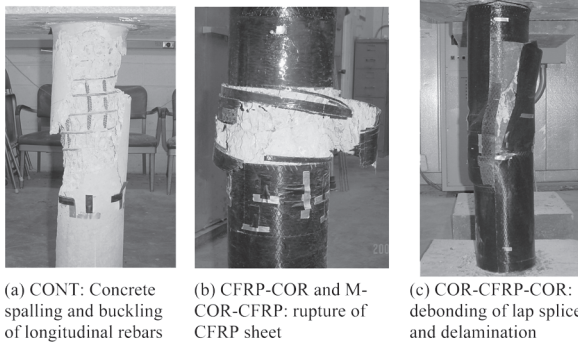


Figure 12—Failure modes of mid-scale RC columns